Model Based Control of Synchronizers for Reducing Impacts during Sleeve to Gear Engagement

Downloaded from: https://research.chalmers.se, 2026-04-04 19:01 UTC

Citation for the original published paper (version of record):
Piracha, M., Grauers, A., Barrientos, E. et al (2019). Model Based Control of Synchronizers for Reducing Impacts during Sleeve to Gear Engagement. SAE Technical Papers, 2019-April(April). http://dx.doi.org/10.4271/2019-01-1303

N.B. When citing this work, cite the original published paper.

research.chalmers.se offers the possibility of retrieving research publications produced at Chalmers University of Technology. It covers all kind of research output: articles, dissertations, conference papers, reports etc. since 2004. research.chalmers.se is administrated and maintained by Chalmers Library

(article starts on next page)

Downloaded from SAE International by Muddassar Piracha, Thursday, March 21, 2019

2019-01-1303 Published 02 Apr 2019

Model Based Control of Synchronizers for Reducing Impacts during Sleeve to Gear Engagement

Muddassar Zahid Piracha Chalmers University of Technology/ CEVT AB

Anders Grauers Chalmers University of Technology

Eva Barrientos, Henrique Budacs, and Johan Hellsing CEVT China Euro Vehicle Technology

Citation: Piracha, M.Z., Grauers, A., Barrientos, E., Budacs, H. et al., "Model Based Control of Synchronizers for Reducing Impacts during Sleeve to Gear Engagement," SAE Technical Paper 2019-01-1303, 2019, doi:10.4271/2019-01-1303.

Abstract

This paper presents a model based control strategy aimed to reduce noise and wear during gearshifts in conventional and hybrid Dual Clutch Transmissions (DCT and DCTH) and Automated Manual Transmissions (AMT). The control strategy is based on a newly developed dog teeth position sensor layout at China Euro Vehicle Technology AB (CEVT), a detailed simulation model for gear engagement and already existing speed sensors in the transmission. The details of dog teeth position sensor and simulation model are also presented in this paper. During gear shifting, noise is generated because of impacts between the sleeve teeth and the idler gear dog teeth after speed synchronization. Besides noise, these impacts are also responsible for delaying the completion of shift and contribute to wear in the dog teeth, hence reducing the lifespan of the transmission. The simulation model for gear engagement can simulate these impacts. Based on the simulation model and optimal control theory, an ideal dog teeth position trajectory is formulated that avoids the impact between sleeve and idler gear dog teeth, before the start of torque ramp up. The open loop strategy then controls the synchronization torque in the beginning of speed synchronization in such a way that the dog teeth position during shift follows the ideal dog teeth position trajectory. Since the control strategy is based on optimal control theory, its effect on speed synchronization time is minimal. The control strategy is designed in such a way that it can easily be applied in the existing transmission control software. By applying the control strategy on the simulation model, it is shown that the impacts during gear engagement are reduced.

Introduction

Throughout the last decades, reducing emissions has been one of the main focus of the automotive industry. Also, the introduction of stricter legislation during the recent years has made the hybridization even more popular. The introduction of electric motors (EM) for traction in the vehicles have significantly reduced the usage of combustion engines (ICE) so vehicles spend more time driving in zero emission mode. ICE is one of the main source of noise in the vehicle. When the usage of ICE is decreased other noise sources in the vehicle which were not deemed important in the past become more emphasized.

This paper deals with noise generation during gear shifting. For gear shifting in hybrid vehicles Dual clutch transmissions (DCT) and automated manual transmissions (AMT) are used. DCT and AMT use conventional synchronization systems, operated by automated shifting actuators [7] and [8].

The high-level gear shifting process can be divided into following phases [7].

1. Torque ramp down
2. Sleeve to Neutral
3. Speed Synchronization
4. Sleeve to Gear Engagement
5. Torque Ramp up

At the beginning of gear shifting during torque ramp down phase, driving torque from ICE or traction EM is removed from off going idler gear. Once the torque is zero, sleeve to neutral phase begins, where sleeve is disengaged from offgoing idler and moved to neutral position. In speed synchronization phase the rotational velocity of oncoming is matched with that of sleeve. Once the speed difference between oncoming idler and sleeve is zero, sleeve to gear engagement phase starts where sleeve is pushed to engage with oncoming idler. After sleeve has moved a certain distance on oncoming idler driving torque from ICE or traction EM is resumed and shift is finished.

The quality of gear shift as perceived by driver is based on the time taken from torque ramp down to torque ramp up [6]. During sleeve to engagement phase, there are impacts between sleeve teeth and idler gear dog teeth [4]. These impacts are responsible for noise during gear shifts in vehicles.

© 2019 SAE International. All Rights Reserved.

Downloaded from SAE International by Muddassar Piracha, Thursday, March 21, 2019

Additionally, these impacts are also responsible for shortening the life span of transmission [4].

A lot of research has been done on dynamic modeling of these impacts as shown in [1] and [3] but research on control system development to avoid these impacts altogether is lacking. In this paper, a control strategy that aims to avoid these impacts is proposed. Since the control strategy aims to avoid impacts, the dynamics during impact are of secondary importance and can easily be included in the simulation models presented in this paper by using the methods explained in [4].

The impacts are explained in [2] which studies dog clutches, but the method can be extended to study of synchronizer systems since the dynamics of dog clutches and synchronizers are same in sleeve to gear engagement phase [4].

The first section of the paper "Simulation Model" describes the speed synchronization and gear engagement phase. In gear engagement phase description, the contacts between sleeve and idler gear dog teeth are classified and the conditions to avoid these contacts are formulated. In second section "AMESim Model" simulations results are presented that demonstrate that the best quality shifts are achieved when the conditions formulated in simulation model are fulfilled. Third section presents a newly proposed sensor layout capable of detecting sleeve dog teeth and idler gear dog teeth and its connection with the control software. Based on the sensor information, an open loop control strategy is proposed in the fourth section. The control strategy controls the gear actuator or electric motor at the beginning of speed synchronization such that the sleeve teeth never impact with idler gear dog teeth before the start of torque ramp up. The effects of control strategy on synchronization time are also discussed.

Simulation Model

The driveline model of DCTH is shown in Figure 1. The integrated electric motor (EM) is shown in dark blue color in Figure 1. EM can give traction torque to the vehicle as well as assist during gear shifting. The gear shift from initial gear ratio to target gear ratio contains two distinct phases.

1. Speed synchronization

FIGURE 1 Driveline model

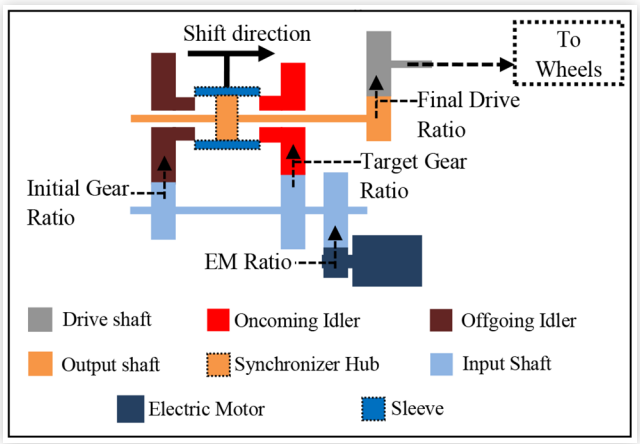

© 2019 SAE International. All Rights Reserved.

Gear Engagement

Speed Synchronization

During speed synchronization, the speed of oncoming idler gear or simply referred to as gear henceforth ω_g is matched with sleeve speed ω_s. As it can be seen from Figure 1, the sleeve is connected to the wheels. In this paper, it is assumed that the shift velocity of vehicle v_{veh} will remain constant during the shift since the vehicle does not have much time to decelerate if the shift is fast. The angular velocity of driveshaft will be

$$\omega_{drive\ shaft} = v_{veh} / R_w \tag{1}$$

where R_w is the wheel radius. From $\omega_{drive\ shaft}$ in equation 1, ω_s can be calculated by

$$\omega_s = \omega_{drive\ shaft} \times Final\ Drive\ Ratio \tag{2}$$

In this paper, the driveshaft is assumed to be infinitely stiff, so there is no torsional degree of freedom between sleeve and wheels.

At the start of speed synchronization at time t_0 the velocity of gear $\omega_g(t_0)$ is calculated by

$$\omega_g(t_0) = \omega_s \times (Initial\ Gear\ Ratio / Target\ Gear\ Ratio) \tag{3}$$

A synchronization torque T_{synch} is then applied on gear such that its velocity at synchronization time t_{synch} is equal to ω_s from equation 2 as shown in Figure 2.

T_{synch} can be provided either by synchronizer ring or by electric motor as explained by [7]. The resulting angular acceleration in oncoming idler α_g is calculated for upshifts by

$$\alpha_g = (-T_{synch} - T_d) / J_g \tag{4}$$

and for downshifts by

$$\alpha_g = (T_{synch} - T_d) / J_g \tag{5}$$

where J_g is the inertia of idler gear, input shaft and electric motor and T_d is the drag torque. Calculation of J_g depends on whether the synchronization is done with synchronizer rings or electric motor as explained by [7].

The synchronization time t_{synch} can be calculated by

$$t_{synch} = \left| \omega_{sg}(t_0) / \alpha_g \right| \tag{6}$$

where $\omega_{sg}(t_0)$ is relative velocity between sleeve and idler gear dog teeth at time t_0 and is calculated by

$$\omega_{sg}(t_0) = \omega_s - \omega_g(t_0) \tag{7}$$

FIGURE 2 Speed synchronization trajectory

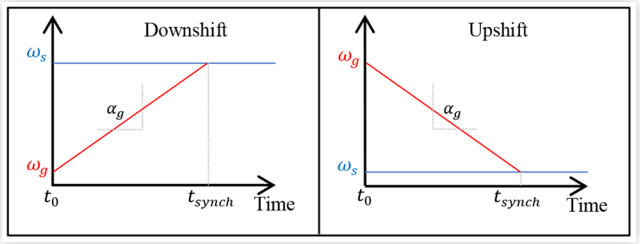

© 2019 SAE International. All Rights Reserved.

© 2019 SAE International. All Rights Reserved.

Downloaded from SAE International by Muddassar Piracha, Thursday, March 21, 2019

Transition between Speed Synchronization and Gear Engagement

Mechanical synchronizer is shown in Figure 3.

Analysis of synchronizers becomes very convenient when each individual component is represented by its teeth as also shown in Figure 3. Throughout paper the teeth representation is used with sleeve teeth in blue, blocker ring teeth in green and idler gear dog teeth in red.

Figure 4 shows speeds and torques on individual teeth during transition between speed synchronization and gear engagement phase. At the end of speed synchronization at time t_{synch} (shown by dashed line in Figure 4), relative velocity between sleeve and oncoming idler $\omega_{sg}(t_{synch})$ is zero. This results in T_{synch} becoming smaller than indexation torque T_I.

This reversal of torque relationship or "ring unblocking" is explained in detail in [9] when the speed synchronization is done by synchronizer rings in synchronizer. If speed synchronization is done by electric motor the torque balancing relationships explained in [9] must still be respected to avoid unblocking before speed synchronization. After the torque reversal, sleeve teeth can push the blocker ring teeth aside and move towards idler gear dog teeth for engagement. Blocking position as explained by [8] is denoted by x_{synch} in Figure 4. Axial force applied on sleeve by actuator mechanism is denoted by F_{ax} and is explained in [7].

FIGURE 3 Mechanical synchronizer and teeth representation

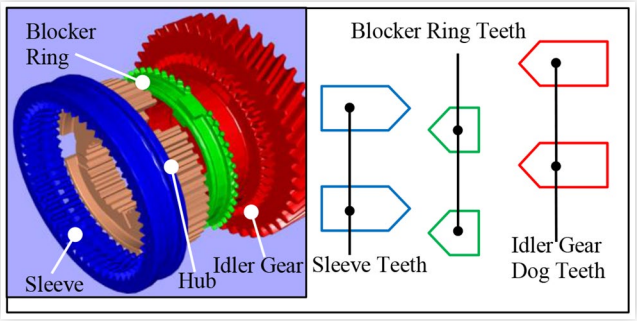

© 2019 SAE International. All Rights Reserved.

FIGURE 4 Unblocking of sleeve teeth

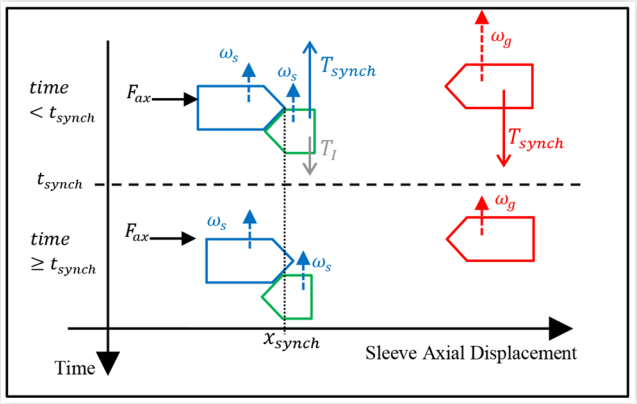

© 2019 SAE International. All Rights Reserved.

In this paper, the sleeve axial velocity $\dot{x}_s$ in gear engagement phase is assumed to be constant. Axial force from actuator mechanism is responsible for maintaining $\dot{x}_s$. Actuator mechanism is designed to have enough axial force to provide clamping torque for synchronizer rings in synchronizers. Compared to that, the axial force required to maintain a constant $\dot{x}_s$ is very small so it's a valid assumption. Based on this assumption, the axial force on actuator will not be discussed in subsequent sections and only $\dot{x}_s$ will be dealt with.

Gear Engagement

At the end of speed synchronization $\omega_s(t_{synch})$ equals $\omega_g(t_{synch})$, but as sleeve moves forward from x_{synch}, synchronization torque T_{synch} on gear disappears as explained in the previous section. Since drag torque is always present, it means that with time after t_{synch} sleeve and gear will go increasingly out of synchronization. To compensate this behavior, a compensation torque T_{comp} is applied on idler gear in the direction of ω_s and opposite to T_d. In DCTH T_{comp} is applied by electric motor and in DCT and AMT it is applied by main clutch. Drag torque although is speed dependent but for such small intervals of time can be estimated to be a constant and its value can be extracted from the methods explained in [5]. The relation between T_{comp}, T_d and $\omega_g(t > t_{synch})$ and ω_s is

$$\omega_g\left(time > t_{synch}\right) is \begin{cases} > \omega_s \; if \; T_{comp} > T_d \\ < \omega_s \; if \; T_{comp} < T_d \\ = \omega_s \; if \; T_{comp} = T_d \end{cases} \tag{8}$$

Teeth Geometry and Coordinate Description Teeth geometry of sleeve and idler gear dog teeth are shown in left half of Figure 5. In this paper, the back angle on teeth is ignored since it affects disengagement and disengagement is not discussed here. It is also assumed that sleeve teeth and idler gear dog teeth have same teeth width w_{dog} and teeth half angle β as shown in Figure 5. The tangential clearance between two meshed teeth is ct and it is measured when sleeve teeth are engaged with idler gear dog teeth as shown by dotted outline of sleeve teeth. The time when engagement is finished is denoted by t_{end} and it is measured when sleeve has traveled

FIGURE 5 Teeth geometry and frame definition

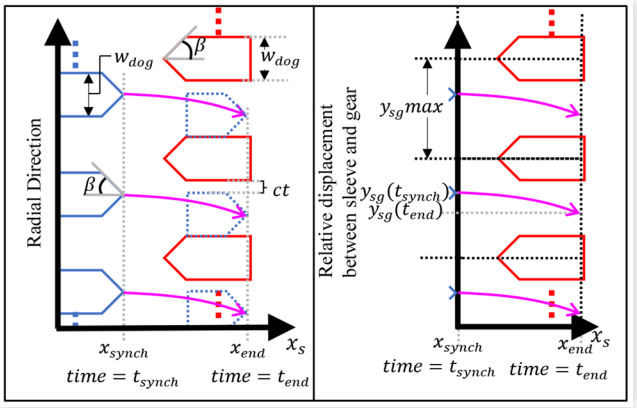

© 2019 SAE International. All Rights Reserved.

Downloaded from SAE International by Muddassar Piracha, Thursday, March 21, 2019

a distance x_{end}. After sleeve has reached x_{end} torque ramp up can start. The trajectory of tip point of sleeve dog is shown by solid magenta curve in Figure 5.

The radial direction that is y-axis of left half of Figure 5 goes from 0 to 360 degrees because sleeve and gear have independent radial movement in the absence of synchronization torque. If the radial direction is divided into windows shown by dotted black rectangle of width x_{synch} to x_{end} and height $y_{sg}max$ such that

$$y_{sg}\max = 2 \times w_{dog} + ct \tag{9}$$

Then the trajectory of tip point of sleeve teeth is same in each window as shown in Figure 5. By using this convention y-axis can be changed to relative displacement between sleeve and idler gear dog teeth y_{sg}, whose limits are between 0 to $y_{sg}max$. Since $y_{sg}max$ is distance between two consecutive teeth tips following holds

$$y_{sg}\max = 2\pi \times R / n_{dog} \tag{10}$$

where R is gear radius or sleeve radius and n_{dog} is number of dog teeth. The relative displacement at time t_{synch}, is denoted by $y_{sg}(t_{synch})$ and at time t_{end} by $y_{sg}(t_{end})$ as shown in Figure 5.

The relationship between T_{comp} and T_d can be used to define the curve of sleeve tip point trajectory at any time instance $t_i \in [t_{synch}, t_{end}]$ before impact with gear teeth.

$$y_{sg}(t_i) = y_{sg}(t_{synch}) - R_g \times 0.5 \times \left\{t_i^2 - t_{synch}^2\right\} \ldots \times \left(T_{comp} - T_d\right) / J_g \tag{11}$$

Assuming that resulting $y_{sg}(t_i) \in [0, y_{sg}max]$ and based on the fact that $\{t_i^2 - t_{synch}^2\}$ term in equation 11 is a positive number since t_i refers to a time later than t_{synch}, following relationship between T_{comp}, T_d, $y_{sg}(t_i)$ and $y_{sg}(t_{synch})$ can be derived from equation 11

$$y_{sg}(t_i)\, is \begin{cases} \left\langle y_{sg}(t_{synch})\ if\ T_{comp} \right\rangle T_d \\ > y_{sg}(t_{synch})\ if\ T_{comp} < T_d \\ = y_{sg}(t_{synch})\ if\ T_{comp} = T_d \end{cases} \tag{12}$$

If $y_{sg}(t_{synch})$ is close to 0 or $y_{sg}max$ then $y_{sg}(t_i)$ might leave the window containing $y_{sg}(t_{synch})$ shown in Figure 5 and will move to an upper or lower window. An example of such a situation where $T_{comp} > T_d$ and $y_{sg}(t_{synch})$ is close to 0 is shown in left half of Figure 6.

As it can be seen in left half of Figure 6, $y_{sg}(t_i)$ calculated by equation 11 denoted by $y_{sg}(t_i)$ goes to the window lower than the one containing $y_{sg}(t_{synch})$. In this case, a new value of $y_{sg}(t_i)$, $Lim\ y_{sg}(t_i)$ is calculated using floor function such that $Lim\ y_{sg}(t_i) \in [0, y_{sg}max]$ by

$$Lim\ y_{sg}(t_i) = y_{sg}\max \times \left[\left(y_{sg}(t_i) / y_{sg}\max\right) - \ldots \left(y_{sg}(t_i) / y_{sg}\max\right)\right] \tag{13}$$

The resulting sleeve tip point trajectory is shown in right half of Figure 6. As it can be seen from dotted blue circles in left half of Figure 6, $Lim\ y_{sg}(t_i)$ and $y_{sg}(t_i)$ are same positions wrt idler gear dog teeth.

FIGURE 6 Relative displacement between sleeve and gear goes outside the limits

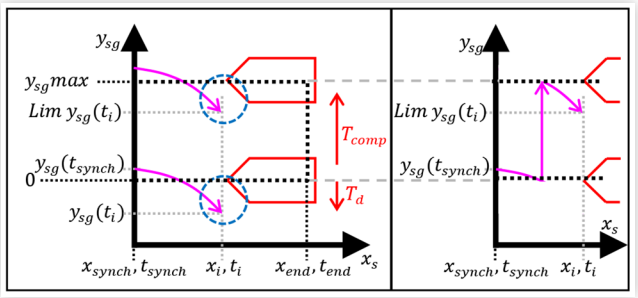

© 2019 SAE International. All Rights Reserved.

Possible Sleeve Tip Point Position during Engagement Phase In this section, the limits in which the sleeve tip point will stay during gear engagement are formulated.

If $T_{comp} = T_d$, then according to equation 11 $\omega_{sg}(t > t_{synch})$ is equal to 0 and equation 12 implies $y_{sg}(t_i)$ is equal to $y_{sg}(t_{synch})$, so the sleeve tip point trajectory will be straight wrt time. Using T_{comp}equal to T_d the sleeve travel from end of speed synchronization till end of gear engagement is shown in Figure 7 from t_{synch} to t_{end} in downwards direction through subfigures a through e. In Figure 7, bouncing back of sleeve by hitting gear dog teeth is not considered since the purpose is to define the limits of area where the sleeve tip point will be and even if the sleeve bounces back it will still be within this area.

For subfigures to the left in Figure 7, $y_{sg}(t_{synch}) = y_{sg}max$ and in the subfigures to the right $y_{sg}(t_{synch}) = 0$. The window of width x_{synch} to x_{end} and height 0 to $y_{sg}max$ is shown by dotted black rectangles in Figure 7a and is repeated in all subfigures. When sleeve starts to move towards engagement with a constant velocity, the front of sleeve will not hit the gear until x_s is larger than or equal to x_{frcnt} as shown in Figure 7b. This movement is referred to in literature as free flight. If sleeve tip point trajectory is seen with respect to gear teeth there is no difference between left and right subfigures in Figure 7a and Figure 7b. There is a difference however when x_s is larger than x_{frcnt} as it can be seen in Figure 7c, where left and right subfigures show sleeve contact with different flanks of gear teeth. The front of sleeve then starts sliding on the gear until x_s is smaller than or equal to x_{sdcnt} as shown in Figure 7d. For x_s larger than x_{sdcnt} the front of sleeve will not be in contact with gear teeth but the side of sleeve can be. The distance between x_{frcnt} and x_{sdcnt} is calculated by

$$x_{sdcnt} - x_{frcnt} = w_{dog} / \tan\beta \tag{14}$$

As shown by left and right subfigures of Figure 7d, value of y_{sg} when x_s is equal to x_{sdcnt} are defined by $y_{sg}sdmax$ and $y_{sg}sdmin$. $y_{sg}sdmax$ and $y_{sg}sdmin$ are limits on y_{sg} if side of sleeve is in contact with the dog teeth and are calculated by

$$y_{sg}sdmin = w_{dog} \tag{15}$$

$$y_{sg}sdmax = w_{dog} + ct \tag{16}$$

Figure 7e shows the sleeve reaching x_{end} from x_{sdcnt}. The sleeve tip point trajectories from all subfigures in Figure 7 when collected together from x_{synch} to x_{end} give the area in

© 2019 SAE International. All Rights Reserved.

Downloaded from SAE International by Muddassar Piracha, Thursday, March 21, 2019

FIGURE 7 Sleeve engagement, showing the two cases, which define the limits for the possible values of y_{sg} as function of x_s

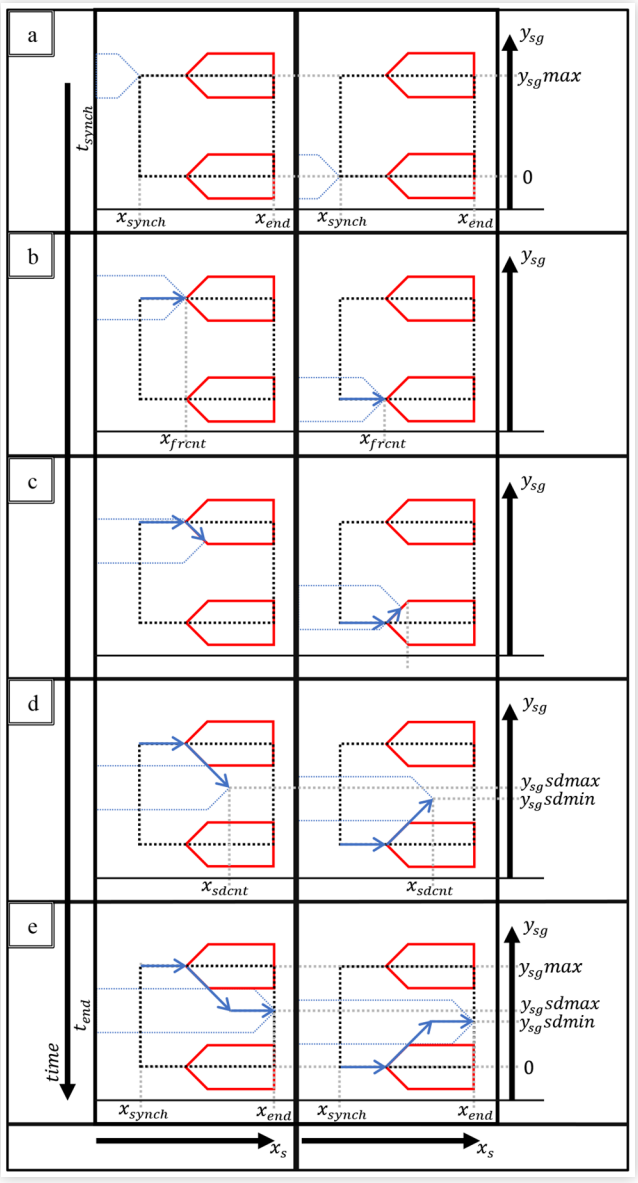

© 2019 SAE International. All Rights Reserved.

which sleeve tip point can exist during gear engagement phase as shown in Figure 8. x_{synch} and x_{frcnt} are defined by synchronizer geometry and x_{end} is defined in transmission control software. Rest of points required for drawing Figure 8, can be derived using equations 10, 14, 15 and 16.

Based on location of sleeve tip point inside the blue area in Figure 8, the kind of contact between sleeve and gear can be described as frontal contact, side contact or no contact.

Frontal Contact. If sleeve tip point trajectory $y_{sg}(t_{synch}, t_{end})$ hits the solid blue line in Figure 8 when $x_s \in [x_{frcnt}, x_{sdcnt}]$, the contact is a frontal contact. This kind of contact produces a force on sleeve that is in the opposite direction of sleeve movement as shown in Figure 7c. The resulting contact force produces a clonk kind of noise and wear in transmission.

© 2019 SAE International. All Rights Reserved.

FIGURE 8 Sleeve tip point trajectory limits

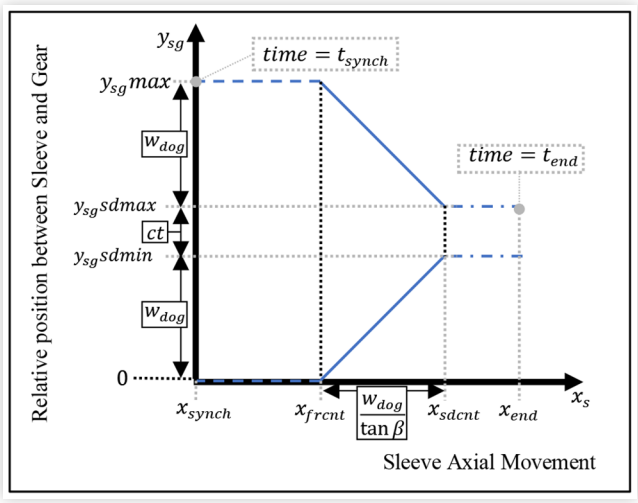

© 2019 SAE International. All Rights Reserved.

Side Contact and Multiple Side Contact. If sleeve tip point trajectory $y_{sg}(t_{synch}, t_{end})$ hits either $y_{sg}sdmin$ or $y_{sg}sdmax$ line in Figure 8 when $x_s \in (x_{sdcnt}, x_{end}]$, the contact is a side contact.

A rattling kind of noise is produced if y_{sg} hits both $y_{sg}sdmin$ and $y_{sg}sdmax$ when $x_s \in (x_{sdcnt}, x_{end}]$. This kind of contact is referred to as multiple side contact.

No Contact or Free Flight. If sleeve tip point trajectory $y_{sg}(t_{synch}, t_{end})$ hits the dashed blue line when $x_s \in [x_{synch}, x_{frcnt})$ or does not hit either solid or dot-dashed blue line, there is no contact between sleeve and gear until the start of torque ramp up. This kind of gear engagement is desired since it does not produce any noise or wear and is fastest.

Ideal Relative Displacement at the End of Engagement $y_{sg}(t_{end})$ Side contact is inevitable when torque ramp up starts, so when x_s becomes equal to x_{end}, $y_{sg}(t_{end})$ will be either $y_{sg}sdmin$ or $y_{sg}sdmax$. The transition between end of engagement and start of torque ramp up is shown in Figure 9.

In left half of Figure 9, at time t_{end} when $x_s = x_{end}$, $y_{sg}(t_{end}) \in [y_{sg}sdmin, y_{sg}sdmax]$. At time instance greater than t_{end}, torque ramp up starts and since the direction of ramp up torque for driving the vehicle is always same as the direction of ω_s, ramp up torque will push the oncoming idler to sleeve as shown in right half of Figure 9. So

$$y_{sg}\left(time > t_{end}\right) = y_{sg}sdmin \tag{17}$$

FIGURE 9 y_{sg} at Torque ramp up

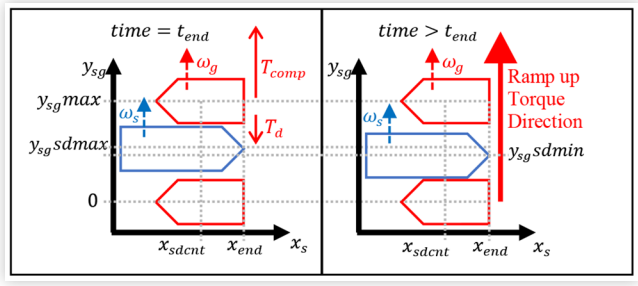

© 2019 SAE International. All Rights Reserved.

Downloaded from SAE International by Muddassar Piracha, Thursday, March 21, 2019

If $y_{sg}(t_{end}) \neq y_{sg}sdmin$, there will be an impact between dog teeth when torque ramp up starts. To avoid this impact

$$y_{sg}\left(t_{end}\right) = y_{sg}sdmin \tag{18}$$

Also, to avoid multiple side contacts the sleeve should never touch the side of the idler gear during engagement, so

$$if\ x_s \in \left(x_{sdcnt}, x_{end}\right] then\ y_{sg} \neq y_{sg}sdmax \tag{19}$$

If direction of ω_s and ω_g are reversed only then y_{sg} for time instance greater than t_{end} would be equal to $y_{sg}sdmax$.

Ideal Relative Displacement at the Start of Engagement $y^*_{sg}\left(t_{synch}\right)$ The ideal starting point for engagement, $y^*_{sg}\left(t_{synch}\right)$ should be calculated such that

1. The resulting sleeve tip point trajectory must not have either frontal or multiple side contact with idler gear dog teeth.
2. The resulting $y_{sg}(t_{end})$ must be as close to $y_{sg}sdmin$ as possible.

Fulfillment of condition 1 guarantees that the gear engagement will be fastest and will be without noise and wear.

Fulfilling the condition 2 above guarantees minimum impact when torque ramp up starts according to equation 17 and 18.

The absence of frontal contact implies there will be no force on sleeve during engagement in the direction opposite to $\dot{x}_s$, the minimum engagement time $t_{end} - t_{synch}$ can then be calculated by

$$t_{end} - t_{synch} = \left(x_{end} - x_{synch}\right) \div \dot{x}_s \tag{20}$$

The velocity difference between sleeve and gear after time $t_{end} - t_{synch}$, will be

$$\omega_s - \omega_g\left(t_{end}\right) = -\left[\left(T_{comp} - T_d\right) \times \left(t_{end} - t_{synch}\right) \div J_g\right] \tag{21}$$

From equation 21, the larger the value of $T_{comp} - T_d$, the larger the velocity difference will be. As mentioned in [2], larger velocity difference leads to more severe impacts, so ideally $T_{comp} - T_d$, must be zero. If it is not zero then the allowable value that guarantees absence of multiple side contacts is defined in the subsequent section.

A time instance t_{sdcnt} can also be defined as time when $x_s = x_{sdcnt}$. It is important to note that time instance t_{sdcnt} does not represent the time instance shown in Figure 7d, because in Figure 7, there is contact between dog teeth. Time $t_{sdcnt} - t_{synch}$ is the time taken for x_s to go from x_{synch} to x_{sdcnt} without frontal contact so

$$t_{sdcnt} - t_{synch} = \left(x_{sdcnt} - x_{synch}\right) / \dot{x}_s \tag{22}$$

The absence of frontal contact also implies that equation 11, can be rewritten for $y_{sg}(t_{end})$ and $y_{sg}(t_{sdcnt})$ as

$$y_{sg}\left(t_{end}\right) = y^*_{sg}\left(t_{synch}\right) - R_g \times 0.5 \times \left\{t_{end}{}^2 - t_{synch}{}^2\right\} \ldots$$

$$\times \left(T_{comp} - T_d\right) / J_g \tag{23}$$

$$y_{sg}\left(t_{sdcnt}\right) = y^*_{sg}\left(t_{synch}\right) - R_g \times 0.5 \times \left\{t_{sdcnt}{}^2 - t_{synch}{}^2\right\} \ldots$$

$$\times \left(T_{comp} - T_d\right) / J_g \tag{24}$$

Subtracting equation 24 from equation 23 results in

$$y_{sg}\left(t_{end}\right) - y_{sg}\left(t_{sdcnt}\right) = -R_g \times 0.5 \times \left\{t_{end}{}^2 - t_{sdcnt}{}^2\right\} \ldots$$

$$\times \left(T_{comp} - T_d\right) / J_g \tag{25}$$

In equation 25, $\{t_{end}{}^2 - t_{sdcnt}{}^2\}$ is always positive, so following relationship between T_{comp}, T_d, $y_{sg}(t_{end})$ and $y_{sg}(t_{sdcnt})$ can be derived as

$$y_{sg}\left(t_{end}\right) is \begin{cases} \left\langle y_{sg}\left(t_{sdcnt}\right) if\ T_{comp} \right\rangle T_d \\ > y_{sg}\left(t_{sdcnt}\right) if\ T_{comp} < T_d \\ = y_{sg}\left(t_{sdcnt}\right) if\ T_{comp} = T_d \end{cases} \tag{26}$$

Equation 26, in combination with equation 18 and constraint 19 can be used to define limits on difference between T_{comp} and T_d, if multiple side contacts is to be avoided. So, if for instance T_{comp} is larger than T_d and $y_{sg}(t_{end})$ is according to equation 18, then if $y_{sg}(t_{sdcnt})$ is less than $y_{sg}sdmax$,multiple side contact can be avoided

$$T_{comp} - T_d = \frac{\left[y_{sg}\left(t_{sdcnt}\right) < y_{sg}sdmax\right] - y_{sg}sdmin}{R_g \times 0.5 \times \left\{t^2_{end} - t^2_{sdcnt}\right\} / J_g} \tag{27}$$

Equation 27 shows if for instance $y_{sg}(t_{sd})$ is chosen to be far smaller than $y_{sg}sdmax$ to keep probability of multiple side contacts very small, then $T_{comp} - T_d$ should be very small , or if $y_{sg}(t_{sd})$ approaches $y_{sg}sdmin$ then $T_{comp} - T_d$ will approach 0 as mentioned by 3rd relation in equation 26.

Equation 21 and 27 define a minimum drag torque compensation $T_{comp} - T_d$ with respect to relative velocity ω_{sg} and relative position y_{sg} at the end of gear engagement independently. The value of $T_{comp} - T_d$ that must be used is minimum of the two results.

Equation 27 also shows the relation between $\dot{x}_s$ and $T_{comp} - T_d$, by $\left\{t^2_{end} - t^2_{sdcnt}\right\}$ term in the denominator. If for instance $\dot{x}_s$ is decreased then according to equation 20 and 22 t_{end} and t_{sdcnt} will increase, making the $\left\{t^2_{end} - t^2_{sdcnt}\right\}$ term increase. In such a scenario if the inequality in 26, is kept unchanged then $T_{comp} - T_d$ must be decreased.

For T_{comp} is less than T_d, $y_{sg}(t_{sd})$ must be less than $y_{sg}(t_{end})$ that is equal to $y_{sg}sdmin$ according to 2nd condition in equation 25, but $y_{sg}sdmin$ is the lowest boundary of y_{sg} when $x_s \in (x_{sdcnt}, x_{end}]$ as shown in Figure 8. So, if direction of ω_s is as shown in Figure 9, T_{comp} must not be smaller than T_d if impact at torque ramp up needs to be avoided.

AMESim Model

Gear engagement model made in *LMS Imagine AMESim* is shown in Figure 10.

The model is initialized at the end of synchronization at time t_{synch} and can be used to see the effects of particular $y_{sg}(t_{synch})$ value on engagement times, frontal contact and possibility of multiple side contacts for specific value of $T_{comp} - T_d$.

Teeth parameters implemented in simulation are shown in Table 1.

The teeth contact parameters in Table 1 are chosen to be nominal values based on experience and are explained in

© 2019 SAE International. All Rights Reserved.

Downloaded from SAE International by Muddassar Piracha, Thursday, March 21, 2019

FIGURE 10 Gear Engagement model

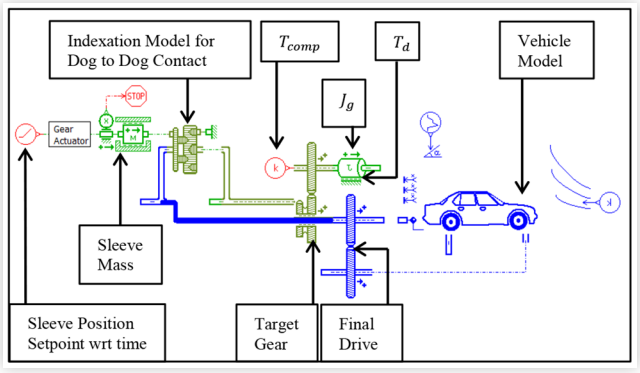

© 2019 SAE International. All Rights Reserved.

TABLE 1 Teeth parameters

Teeth Geometry Parameters	
w_{dog}	4 mm
ct	0.5 mm
β	45 degrees
$y_{sg}max$	8.5 mm
$y_{sg}sdmin$	4 mm
$y_{sg}sdmin$	4.5 mm
$x_{frcnt} - x_{synch}$	2 mm
$x_{sdcnt} - x_{frcnt}$	4 mm
$x_{end} - x_{synch}$	8 mm
$\dot{x}_s$	500 mm/sec
Teeth contact Parameters	
Stiffness of teeth for contact	1e10 N/m
Damping of teeth for contact	1e4 N/m/s
Limit penetration for contact	1e-3 mm
Viscous friction for contact	5 N/m/s
Friction coefficient for contact	0.3

© 2019 SAE International. All Rights Reserved.

[2]. Accurate values of these parameters can be calculated by the experimental method shown in [4]. The consequence of not using accurate values will be that the contact forces will not be accurate but the relative magnitude of contact forces resulting from different $y_{sg}(t_{synch})$ will still be the same. Hence the relative level of noise generated by different frontal contacts can be evaluated. Using this approach multiple side contacts and consequent rattling noise cannot be evaluated. But the potential of multiple side contacts resulting from different $y_{sg}(t_{synch})$ can still be evaluated.

Simulation Results

Using teeth parameters given in Table 1,value of $T_{comp} - T_d$ equal to 19Nm satisfies equation 27 with $y_{sg}(t_{sdcnt}) + 1mm$ equal to $y_{sg}sdmax$ as shown by the dotted magenta curve in Figure 11.

In Figure 11, x axis is from 0 to 8mm, where for sake of simplicity x_{synch} is assumed to be 0 and then x_{end} is 8mm according to Table 1. Using equation 21, $T_{comp} - T_d$ equal to 19Nm results in $\omega_{sg}(t_{end})$ equal to -2rad/sec. Any value of $T_{comp} - T_d \in [0, 19Nm)$ will satisfy equation 27 and lead to $\omega_{sg}(t_{end}) \in (-2rad/sec, 0]$. Using a lower value $T_{comp} - T_d$ equal

© 2019 SAE International. All Rights Reserved.

FIGURE 11 Sleeve tip point trajectory with $y^*_{sg}(t_{synch})$

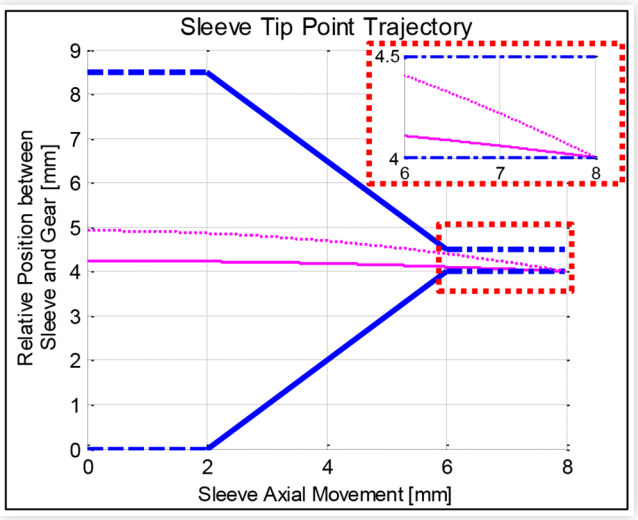

© 2019 SAE International. All Rights Reserved.

to 5Nm leads to $\omega_{sg}(t_{end})$ equal to -0.5rad/sec and results to $y^*_{sg}(t_{synch})$ to be 4.245mm as shown by solid magenta curve Figure 11.

A batch simulation is run on the model shown in Figure 12 such that $y_{sg}(t_{synch})$ for all simulations is changing from 1.245mm till 7.245mm with a step of 0.2mm.

Since the batch simulation is run with a constant $T_{comp} - T_d$ equal to 5Nm, $y^*_{sg}(t_{synch})$ will be 4.245mm. The resulting sleeve tip point trajectories are shown in Figure 12.

In Figure 12 all trajectories that imply a frontal contact with sleeve are in red or orange curves. Sleeve tip point trajectory for $y^*_{sg}(t_{synch})$ and $y^*_{sg}(t_{synch}) + 0.2mm$ does not make a frontal contact so they are shown in magenta color. A zoomed in view of Figure 12 with selected batch runs is shown in Figure 13.

From Figure 13, it can be seen that $y_{sg}(t_{end})$ for the trajectory generated by $y_{sg}(t_{synch})$ equal to 4.265mm shown by dotted

FIGURE 12 Sleeve tip point trajectories from batch simulation

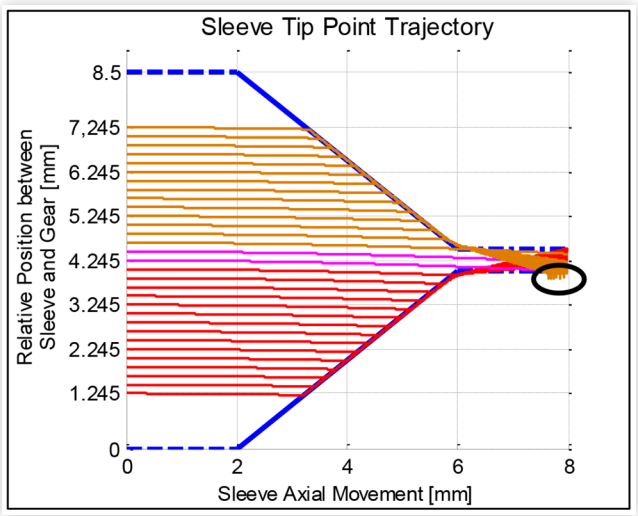

© 2019 SAE International. All Rights Reserved.

Downloaded from SAE International by Muddassar Piracha, Thursday, March 21, 2019

FIGURE 13 Selected Batch simulation results

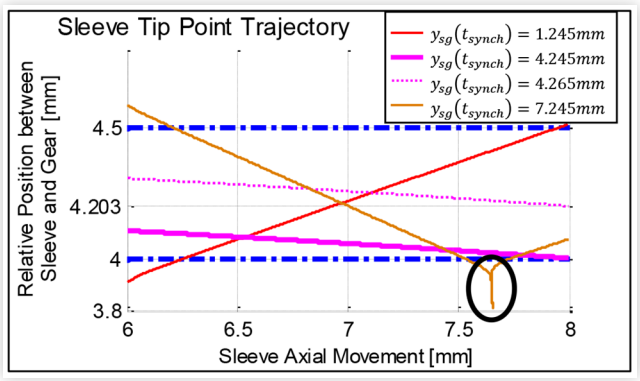

© 2019 SAE International. All Rights Reserved.

magenta curve is not according to equation 18 . The trajectories generated by $y_{sg}(t_{synch})$ equal to 1.245mm and 7.245mm shown in red and orange respectively will have more potential of multiple side contacts and rattling noise according to the criteria described before.

Since T_{comp} is larger than T_d so according to equation (8) ω_g is larger than ω_s after synchronization. With directions of ω_g and ω_s shown by Figure 9, it can be concluded that frontal contacts made by red trajectories in Figure 12 will be more severe because in that case the sleeve hits the idler gear that is approaching it. The frontal contacts made by the orange trajectories is such that the idler gear is moving away from the sleeve. Since the magnitude of frontal force defines the friction between sleeve and gear, so in general red trajectories have more gear engagement time as compared to orange trajectories. The resulting gear engagement times are shown in Figure 14 on y-axis for each $y_{sg}(t_{synch})$ on x-axis.

From Figure 14, gear engagement times for red trajectories in Figure 12 are higher than the orange trajectories. Furthermore, it can be concluded that $y^*_{sg}\left(t_{synch}\right) = 4.245mm$ leads to the fastest gear engagement.

Maximum frontal contact force for the selected batch runs in Figure 12 is shown in Figure 15.

It can be seen from Figure 15 that the contact force is higher for $y_{sg}(t_{synch})$ equal to 1.245mm than it is for $y_{sg}(t_{synch})$ equal to 7.245mm as discussed earlier. Also, the small-time scale and large value of contact force in Figure 15 indicates that the contact force will generate a clonk kind of noise. Maximum value of frontal contact force for all batch simulations shown

FIGURE 14 Gear engagement times from Batch Simulation

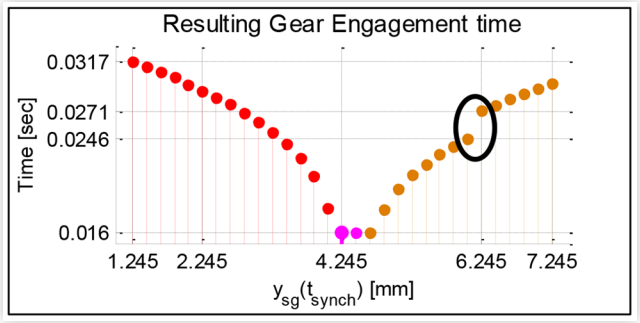

© 2019 SAE International. All Rights Reserved.

FIGURE 15 Frontal contact force for selected batch simulations

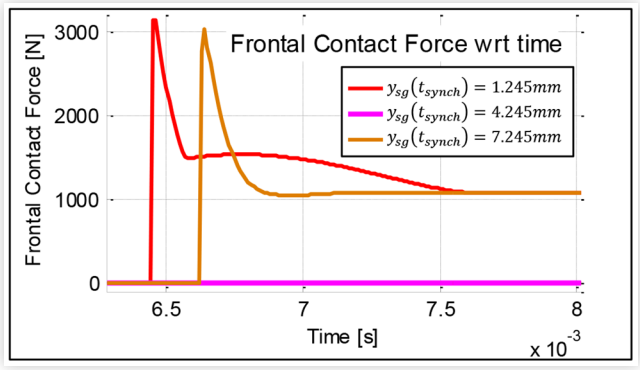

© 2019 SAE International. All Rights Reserved.

in Figure 12 are shown on y-axis in Figure 16 with corresponding values of $y_{sg}(t_{synch})$ shown on x-axis.

From Figure 14 and Figure 16 it can be seen that trajectories from $y_{sg}(t_{synch})$ values less than $y^*_{sg}\left(t_{synch}\right)$ start giving frontal contacts and hence clonk noise as well as delayed gear engagement within $y^*_{sg}\left(t_{synch}\right) - 0.2mm$ but for $y_{sg}(t_{synch})$ values larger $y^*_{sg}\left(t_{synch}\right)$ than the clonk noise and delayed gear engagement shows up after $y^*_{sg}\left(t_{synch}\right) + 0.4mm$. This kind of analysis can thus be used to define the tolerance level with which $y^*_{sg}\left(t_{synch}\right)$ must be controlled in either direction.

The existence of multiple side contacts is shown in Figure 17 for all batch simulations in Figure 12. On y-axis in Figure 17 is the true/false of whether more than one side contact occur for the corresponding $y_{sg}(t_{synch})$ on x -axis.

From Figure 17 it can be seen multiple side contact and hence more probability of rattling exists when $y_{sg}(t_{synch})$ is far from $y^*_{sg}\left(t_{synch}\right)$.

FIGURE 16 Maximum frontal contact force for Batch simulation

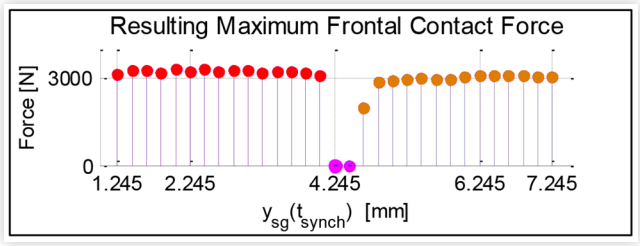

© 2019 SAE International. All Rights Reserved.

FIGURE 17 Existence of multiple side contacts for batch simulations

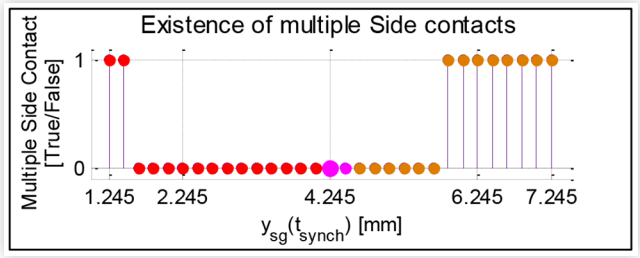

© 2019 SAE International. All Rights Reserved.

© 2019 SAE International. All Rights Reserved.

Downloaded from SAE International by Muddassar Piracha, Thursday, March 21, 2019

From the trajectory for $y_{sg}(t_{synch})$ equal to 7.245mm in Figure 13 it can be seen that when x_s is approximately 7.65mm, marked by the black circle, the sleeve teeth are pushing so hard against the gear teeth, that the simulation result shows a material penetration of about 0.2mm. Same behavior can be seen for trajectories resulting from other values of $y_{sg}(t_{synch})$ as shown by black circle in Figure 12. High side contact force increases the friction between sleeve and gear hence delaying the gear engagement as shown by the sudden increase in gear engagement time marked by black circle in Figure 14. But since the delay it generates is small (of the order of few ms) as compared to delays generated because of frontal contacts (of the order of 10ms) it can be ignored. This phenomenon can be studied in further detail by making the teeth contact parameters given in Table 1 more accurate.

Conclusion from Simulation Results

Based on the simulation results it can be concluded that if the drag torque compensation $T_{comp} - T_d$ is 5Nm, $y^*_{sg}\left(t_{synch}\right) = 4.245mm$ results in minimum gear engagement times, zero frontal contact forces, less probability of multiple side contacts and $y_{sg}(t_{end})$ being equal to $y_{sg}sdmin$, subsequently leading to best shift quality with least noise and wear.

Dog Teeth Position Sensor

Physical Layout of Dog Teeth Position Sensor

To be able to start the engagement at the ideal y^*_{sg} the gear shift controller must have information about the position of the gear sleeve relative to the idler gear dog teeth. To measure that, position sensors must be positioned in a way that sleeve and idler gear dog teeth can be read. On the shift forks, the sleeve teeth position sensor is added as shown in Figure 18, in red.

Since the sleeve teeth are internal, reading marks are made on the outer surface of sleeve which are aligned with the inner dog teeth positions as shown in Figure 19.

The sensor for idler gear dog teeth is added to fork rod as shown in Figure 20, but its position may differ for different transmission concepts. The idler gear dog teeth sensor must always be at a fixed position in space.

FIGURE 18 Sleeve teeth position sensor added to shift fork

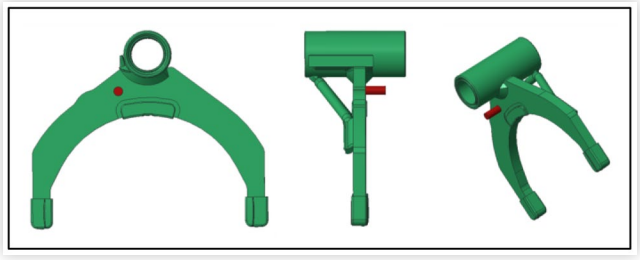

© 2019 SAE International. All Rights Reserved.

FIGURE 19 Reading marks on sleeve

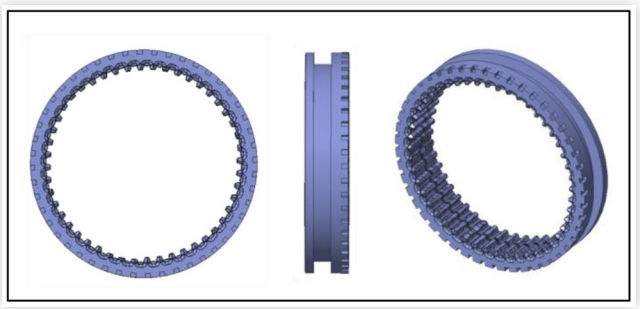

© 2019 SAE International. All Rights Reserved.

FIGURE 20 Idler gear dog teeth position sensor added to shift fork

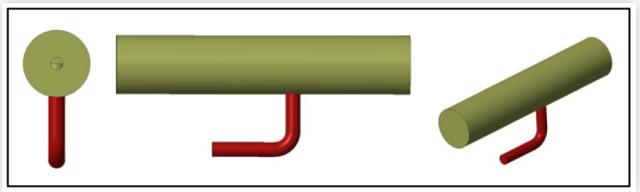

© 2019 SAE International. All Rights Reserved.

FIGURE 21 Synchronizer with added teeth position sensors

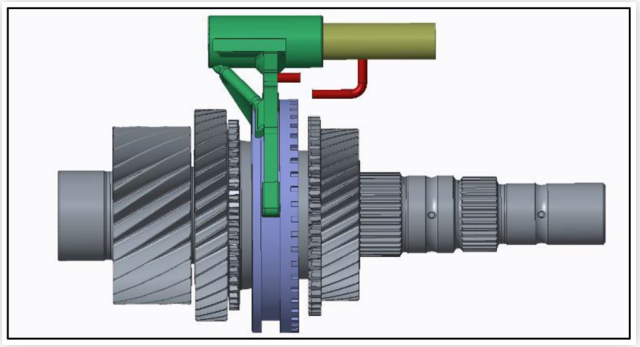

© 2019 SAE International. All Rights Reserved.

The complete assembly of sensors, synchronizer, shift fork and rod is shown in Figure 21.

Signal Processing for Position Sensor

The sensor produces a binary signal i.e. 0 for no teeth and 1 for teeth as shown in Figure 22. Since there are two similar sensors, one for sleeve teeth and one for idler gear dog teeth, signal processing for idler gear dog teeth sensor will be shown here, the signal processing for sleeve teeth sensor will be exactly same.

If idler gear dog teeth are moving in the direction of rotation as shown in Figure 22, the sensor gives rising edges at times t_1 and t_3 and falling edges at times t_2 and t_4. The teeth position $y_g$at time t_1 as shown in Figure 22 would be

$$y_g\left(t_1\right) = y_g \max - w_{dog} / 2 \tag{28}$$

© 2019 SAE International. All Rights Reserved.

Downloaded from SAE International by Muddassar Piracha, Thursday, March 21, 2019

where $y_g max$ is same as $y_{sg} max$ and is defined by equations 9 and 10. Similarly, teeth position at time t_2 would be

$$y_g(t_2) = w_{dog}/2 \tag{29}$$

Values of y_g between time t_1 and time t_2 can be calculated by

$$y_g\left(t \in [t_1, t_2]\right) = R \times \left(\int \omega_g dt + y_g(t_1)/R\right) \tag{30}$$

If y_g resulting from equation 30 is not between 0 and $y_{sg} max$ equation 13 is applied to make it so.

Similarly values of y_g between time t_2 and t_3 can be calculated by

$$y_g\left(t \in [t_2, t_3\right) = R \times \left(\int \omega_g dt + y_g(t_2)/R\right) \tag{31}$$

For values of y_g between times t_3 and t_4 equation 30 can be used again. In essence y_g at any time can be calculated by integrals in equations 30 and 31, which are triggered by either a rising or a falling edge and reset by the other.

If direction of rotation or equivalently sign of ω_g is changed in Figure 22, then falling edges will be at times t_1 and t_3 and rising edges at times t_2 and t_4. In that case the triggers for integral equations 30 and 31 must be interchanged.

The logic implemented in Simulink is shown in Figure 23.

In Figure 23, the first *If Then Else* block shown in red changes the trigger conditions between the integrators based on sign of angular velocity. Second *If Then Else* block activates the integrator blocks based on rising or falling edges in sensor signal and integrates the velocity signal with respective initial conditions. The resulting y_g from a decreasing ω_g and corresponding sensor signal is shown in Figure 24.

FIGURE 22 Sensor output and teeth position

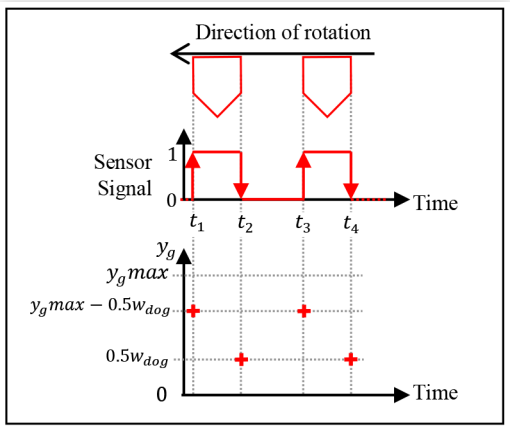

© 2019 SAE International. All Rights Reserved.

FIGURE 23 Algorithm for Dog teeth position from velocity and sensor signal

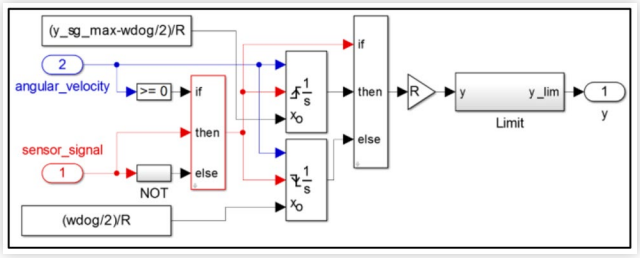

© 2019 SAE International. All Rights Reserved.

FIGURE 24 Resulting y_g from $\omega_g = 40 \rightarrow 0$ rad/sec

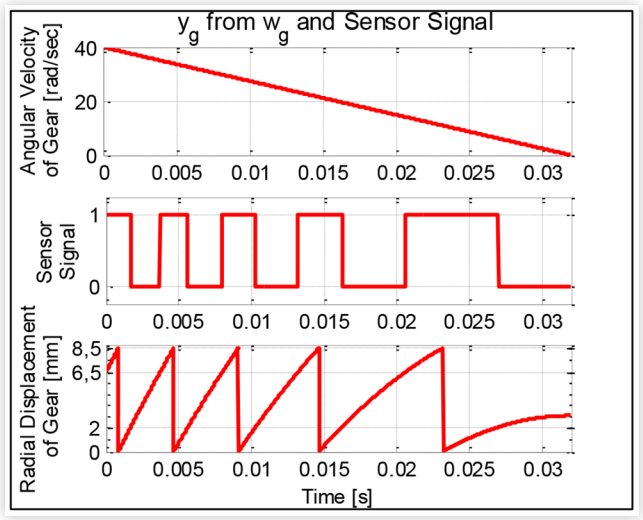

© 2019 SAE International. All Rights Reserved.

It can be seen in Figure 24, that the rising and falling edges of sensor signal are in accordance with Figure 22 and dog teeth parameters from Table 1.

Similar logic can be used to get sleeve teeth position y_s at any time based on the sensor signal for sleeve teeth and sleeve velocity ω_s. Based on y_s and y_g, the real relative displacement between sleeve teeth and idler gear dog teeth y_{sgr} at any time instance t_i can be calculated by

$$y_{sgr}(t_i) = \begin{cases} y_g(t_i) - y_s(t_i) \; if \; y_g(t_i) > y_s(t_i) \\ y_{sg}\max - y_s(t_i) + y_g(t_i) \; if \; y_s(t_i) > y_g(t_i) \end{cases} \tag{32}$$

The resulting y_{sgr} will be a sawtooth wave like radial displacement plot in Figure 24.

Gear Engagement Control Algorithm

The control algorithm is applied in beginning of the speed synchronization phase and the aim of the algorithm is to make y_{sgr} at end of speed synchronization, at time t_{synch} equal to $y^*_{sg}(t_{synch})$.

Ideal Relative Displacement at Start of Synchronization $y_{sg1}(t_0)$

Ideal relative displacement between sleeve teeth and idler gear dog teeth at the start of speed synchronization $y_{sg1}(t_0)$ corresponds to a particular value of displacement such that when a maximum angular acceleration α_g is applied at time t_0, relative displacement after time t_{synch}, is equal to $y^*_{sg}(t_{synch})$. Maximum value of angular acceleration $Max(\alpha_g)$ can be calculated corresponding to a maximum synchronization torque T_{synch} according to equation 4 or 5.

© 2019 SAE International. All Rights Reserved.

Downloaded from SAE International by Muddassar Piracha, Thursday, March 21, 2019

$y_{sg1}(t_0)$ can be calculated by assuming $y_{sgr}(t_{synch})$ being equal to $y^*_{sg}(t_{synch})$. Under this assumption values of y_g and y_s measured by the dog teeth position sensor at time t_{synch} will be such that

$$y_g(t_{synch}) = y^*_{sg}(t_{synch}) \tag{33}$$

$$y_s(t_{synch}) = 0 \tag{34}$$

then according to first condition in equation 32 $y_{sgr}(t_{synch})$ is equal to $y^*_{sg}(t_{synch})$.

From equation 33 angular displacement of gear θ_g at time t_{synch} can be calculated to be

$$\theta_g(t_{synch}) = y^*_{sg}(t_{synch}) / R_g \tag{35}$$

Similarly, from equation 34 angular displacement of sleeve θ_s at time t_{synch} can be calculated to be

$$\theta_s(t_{synch}) = 0 \tag{36}$$

To calculate $y_{sg1}(t_0)$ a simulation running backwards in time from time t_{synch} to time t_0 with a small decremental step of δt is shown in Figure 25.

The initial conditions for the angular displacements θ_g and θ_s for the simulation are equations 35 and 36 respectively. Initial condition for ω_g is $\omega_g(t_{synch}) = \omega_s$. When the simulation stops after $(t_{synch} - t_0)/\delta t$ iterations as shown in Figure 25 the results are collected and post processed to get $\omega_{sg}(t), \forall\, t \in [t_0, t_{synch}]$ and $y_{sg1}(t), \forall\, t \in [t_0, t_{synch}]$. The curve $y_{sg1}(t)$ is post processed in such a way that $y_{sg1}(t_0) \in [0, y_{sg}max]$ and $Lim\ y_{sg1}(t_{synch})$ calculated by equation 13 is equal to $y^*_{sg}(t_{synch})$.

Phase plane trajectory generated for an upshift with $\omega_{sg}(t_0) = -100\ rad/sec$ and $y^*_{sg}(t_{synch}) = 4.245mm$ is shown in Figure 26.

Since calculation of $y^*_{sg}(t_{synch})$ is offline, $y_{sg1}(t)$ can also be calculated offline and then implemented as a calibration in the transmission software.

FIGURE 25 Backwards in time simulation

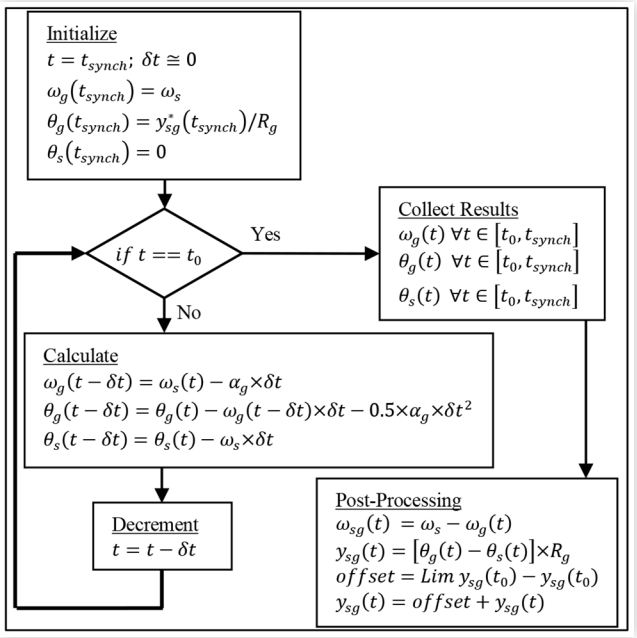

© 2019 SAE International. All Rights Reserved.

© 2019 SAE International. All Rights Reserved.

FIGURE 26 Phase plane trajectory with Maximum α_g for $\omega_{sg}(t_0) = -100\ rad/sec$ and $y^*_{sg}(t_{synch}) = 4.245mm$

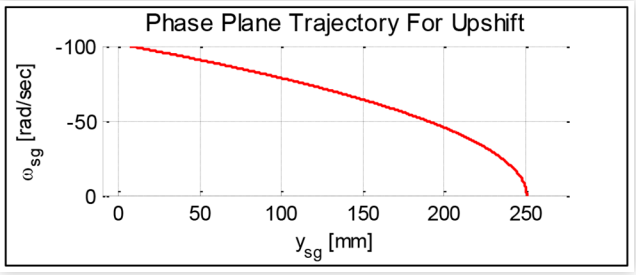

© 2019 SAE International. All Rights Reserved.

Control Logic

The purpose of the control logic is to start speed synchronization when y_{sgr} is equal to $y_{sg1}(t_0)$. So, the control logic will be

$$\alpha_g\ is \begin{cases} = 0\ if\ y_{sgr}\ from\ Sensor \neq y_{sg1}(t_0) \\ = \max(\alpha_g)\ if\ y_{sgr}\ from\ Sensor = y_{sg1}(t_0) \end{cases} \tag{37}$$

The block diagram for controller is shown in Figure 27.

Since the angular acceleration α_g in equation 37 is controlled by synchronization torque T_{synch}, the interface of control logic with the hardware is in terms of T_{synch}. The implementation of open loop control for an upshift in Figure 27 is shown in Figure 28.

FIGURE 27 Controller block diagram

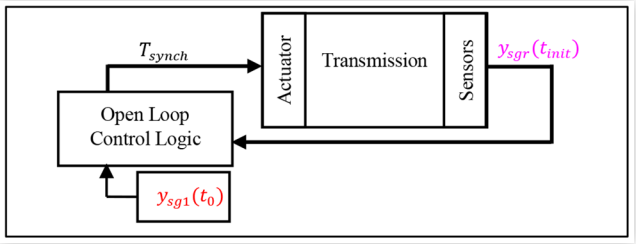

© 2019 SAE International. All Rights Reserved.

FIGURE 28 Open loop control logic for upshifts

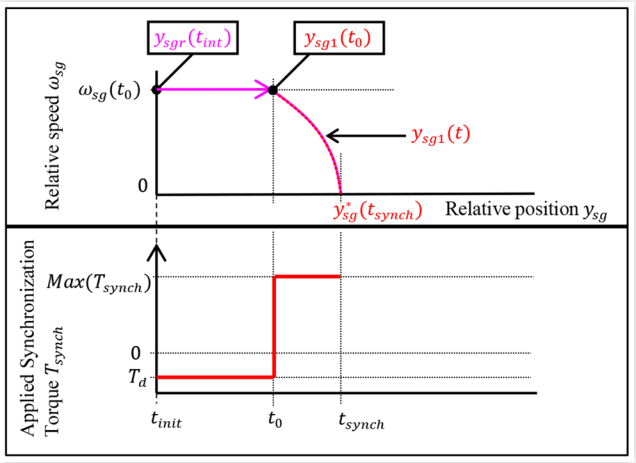

© 2019 SAE International. All Rights Reserved.

Downloaded from SAE International by Muddassar Piracha, Thursday, March 21, 2019

It can be seen from Figure 28 that for time duration t_{int} to t_0, T_{synch} is kept at T_d, which gives α_g=0 according to equation 4. At time instance t_0, when maximum torque is applied y_{sgr} will start following the trajectory y_{sg1}. After time t_{synch}, $\omega_{sg}(t_{synch})$ will be 0 and $Lim\ y_{sgr}(t_{synch})$ will be equal to $Lim\ y_{sg1}(t_{synch})$ which is equal to $y^*_{sg}(t_{synch})$ as mentioned earlier.

Since $y_{sgr}(t_0)$ and $y_{sg1}(t_0)$ both $\in[0, y_{sg}max]$, it is not necessary that $y_{sgr}(t_0)$ is greater than $y_{sg1}(t_0)$ as shown in Figure 28. In that case the y_{sg1} trajectory need to be offset by $y_{sg}max$. So

$$if\ y_{sgr}(t_0) > y_{sg1}(t_0)$$

$$then\ offset\ y_{sg}(t) = y_{sg}(t) + y_{sg}\max \tag{38}$$

Using equation 13 on *offset* $y_{sg}(t)$ at time=t_{synch} from equation 38, it can be calculated that *Lim offset* $y_{sg1}(t)$ is still $y^*_{sg}(t_{synch})$. The offset phase plane is shown by dotted line and original phase plane is shown by solid lines in Figure 29

So, if $y_{sgr}(t_{init})$ is greater than $y_{sg1}(t_0)$, then *offset* y_{sg1} trajectory will be followed after time t_0 instead of y_{sg1} as explained earlier.

Since during time duration t_0–t_{init}, α_g is equal to zero, the speed synchronization is delayed by this duration. So, speed synchronization trajectory shown for upshift in Figure 2 will be updated as shown in Figure 30.

Time duration t_0–t_{init} can be calculated by

$$t_0\text{–}t_{init} = \Delta y_{sg} / \left[R_g \times \omega_{sg}(t_0)\right]$$

where Δy_{sg} = …

$$\ldots \begin{cases} y_{sg1}(t_0) - y_{sgr}(t_{init})\ if\ y^*_{sg}(t_0) > y_{sg}R(t_{init}) \\ y_{sg}\max + y_{sg}(t_0) - y_{sgr}(t_{init})\ if\ y^*_{sg}(t_0) < y_{sg}R(t_{init}) \end{cases} \tag{39}$$

It can be seen from equation 39, that time duration t_0–t_{init} is quiet small since the numerator term Δy_{sg} can be maximum equal to $y_{sg}max$ and denominator contains terms R_g and $\omega_{sg}(t_0)$ which are far larger than Δy_{sg}.

Simulation Results for Open Loop Controller

The simulation results for $y_{sgr}(t_{init}) = 0; 2; 4; 8.4mm$ are shown in Figure 31a. Figure 31b shows the zoom in view of Figure 31a at time t_0 and Figure 31c shows the zoomed in view at time t_{synch}.

From Figure 26, $y_{sg1}(t_0)$ is 7.238mm and $y_{sg1}(t_{synch})$is 250.746mm as shown in Figure 31b and Figure 31c respectively . Since $y_{sgr}(t_{init})$ equal to 8.4mm is larger than $y_{sg1}(t_0)$ so the phase plane for $y_{sgr}(t_{init})$ equal to 8.4mm shown in green follows the offset trajectory shown by dotted red line in Figure 31. Using equation 13 it can be calculated that $Lim\ y_{sg1}(t_{synch})$ is 4.245mm which is $y^*_{sg}(t_{synch})$ calculated in the previous sections. From Figure 31b it can be seen that for different values of $y_{sgr}(t_{init})$, the control algorithm makes sure that y_{sgr} at time t_{synch}, converge to $y^*_{sg}(t_{synch})$, as shown in Figure 31c.

The open loop controller guarantees y_{sgr} at time t_{synch} is equal to $y^*_{sg}(t_{synch})$ by changing y_{sgr} at time t_0 to a fixed $y_{sg1}(t_0)$. But during the time interval t_0 to t_{synch}, y_{sgr} can be controlled by a closed loop controller if dog teeth position sensor is not accurate enough or time interval t_0–t_{init} is too small for the synchronization torque to switch. The closed loop controller that calculates synchronization torque T_{synch}, such that the error between $y_{sgr}(t)$ and $y_{sg1}(t)$ is zero $\forall t \in [t_0, t_{synch}]$ will be a topic for future research.

FIGURE 29 Offset phase plane trajectory

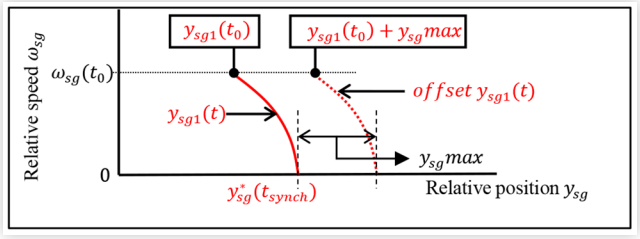

© 2019 SAE International. All Rights Reserved.

FIGURE 30 Upshift speed synchronization trajectory after application of open loop control

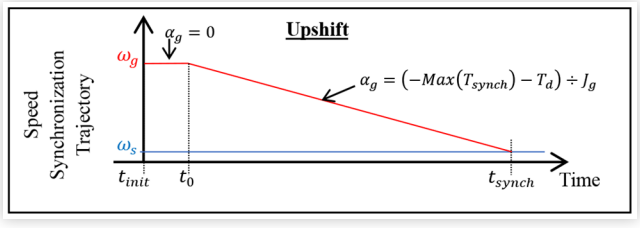

© 2019 SAE International. All Rights Reserved.

FIGURE 31 Open loop control simulation

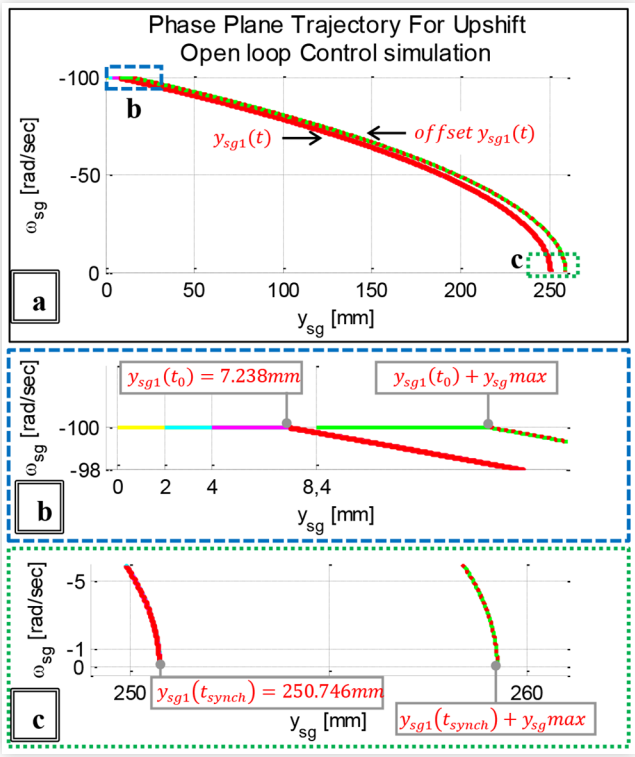

© 2019 SAE International. All Rights Reserved.

© 2019 SAE International. All Rights Reserved.

Downloaded from SAE International by Muddassar Piracha, Thursday, March 21, 2019

Conclusions

This paper has presented a detailed analysis of impacts between sleeve and idler gear dog teeth in gear engagement phase. The exact conditions to avoid these contacts are also formulated. The simulation results from AMESim model demonstrate that impacts can be avoided by fulfillment of before mentioned conditions. If the conditions are not fulfilled the adverse effects on gear engagement are also shown.

A newly proposed dog teeth position sensor is also discussed. The sensor together with already existing velocity sensors can be used to control speed synchronization phase in such a way that dog teeth impacts during gear engagement phase can be avoided. The delay that the control strategy introduces in speed synchronization phase is also proven to be negligible.

References

1. Chen, H. and Tian, G., "Modeling and Analysis of Engaging Process of Automated Mechanical Transmissions," *Multibody System Dynamics* 37:345-369, 2016, doi:10.1007/s11044-015-9490-7.
2. Duan, C., "Analytical Study of a Dog Clutch in Automatic Transmission Application," *SAE Int. J. Passeng. Cars - Mech. Sys.* 7(3):1155-1162, 2014, doi:10.4271/2014-01-1775.
3. Hoshino, H., "Analysis on Synchronization Mechanism of Transmission," in *1999 Transmission and Driveline Systems Symposium*, 1999, SAE.
4. Lu, Z., Chen, H., Wang, L., and Tian, G., "The Engaging Process Model of Sleeve and Teeth Ring with a Precise, Continuous and Nonlinear Damping Impact Model in Mechanical Transmissions," SAE Technical Paper 2017-01-2443, 2017, doi:10.4271/2017-01-2443.
5. Math, K.M.H., and Lund, M., "Drag Torque and Synchronization Modelling in a Dual Clutch Transmission," Master thesis, 2018, Chalmers University of Technology, Gothenburg, Sweden.
6. Penta, A., Gaidhani, R., Kumar Sathiaseelan, S., and Warule, P., "Improvement in Shift Quality in a Multi Speed Gearbox of an Electric Vehicle Through Synchronizer Location Optimization," SAE Technical Paper 2017-01-1596, 2017, doi:10.4271/2017-01-1596.
7. Piracha, M.Z., Grauers, A., and Hellsing, J., "Improving Gear Shift Quality in a PHEV DCT with Integrated PMSM," CTI Symposium Automotive Transmissions, HEV and EV Drives, 2017, CTI, Berlin, http://publications.lib.chalmers.se/records/fulltext/254760/local_254760.pdf.
8. Tseng, C.-Y. and Chih-Hsien, Y., "Advanced Shifting Control of Synchronizer Mechanisms for Clutchless Automatic Manual Transmission in an Electric Vehicle," *Mechanism and Machine Theory* 84:37-56, 2015, doi:10.1016/j.mechmachtheory.2014.10.007.
9. Walker, P.D. and Zhang, N., "Engagement and Control of Synchronizer Mechanisms in Dual Clutch Transmissions," *Journal of Mechanical Systems and Signal Processing* 26:320-332, 2012, doi:10.1016/j.ymssp.2011.07.016.

Contact Information

Muddassar Zahid Piracha
muddassar.piracha@cevt.se
+46 721 84 39 70

© 2019 SAE International. All rights reserved. No part of this publication may be reproduced, stored in a retrieval system, or transmitted, in any form or by any means, electronic, mechanical, photocopying, recording, or otherwise, without the prior written permission of SAE International.

Positions and opinions advanced in this work are those of the author(s) and not necessarily those of SAE International. Responsibility for the content of the work lies solely with the author(s).

ISSN 0148-7191